An experimental investigation on pressure response and phase transition of supercritical carbon dioxide releases from a small-scale pipeline

Xingqing Yan[a], Hailong Zhu[a], Jianliang Yu[a] *, Shaoyun Chen[b], Haroun Mahgerefteh[c]

[a] School of Chemical Machinery and Safety, Dalian University of Technology, Dalian, 116024, China

[b] School of Chemical Engineering, Dalian University of Technology, Dalian, 116024, China

[c] Department of Chemical Engineering, University College London, London WC1E 7JE, UK

Abstract: The prediction of the pressure response and phase transition in the event of an accidental carbon dioxide (CO_2) release from a ruptured pipeline is of significant importance for understanding the depressurization behaviour and hence the fracture behaviour. This article presented a small-scale experimental investigation on the pressure response and phase transition of supercritical CO_2 release from a pressurized pipeline with a relief orifice. High-frequency transducers and thermocouples were used to measure the evolution of CO_2 pressures and temperatures at different locations after release. The results indicated that pressures at different locations decreased nearly synchronously after release. No vapour bubble and pressure rebound generated in larger-scale release experiments were found in our small-scale release experiments. The depressurization rate was greatly affected by the phase transition. During the release process, the supercritical CO_2 firstly turned into an unstable gas with a very great depressurization rate, then changed into the gas–liquid phase with a lower depressurization rate, and finally changed

* Corresponding author: Tel.: +86-411-84986281; Fax: +86-411-84986281.

E-mail address: yujianliang@dlut.edu.cn (J. Yu)

into gaseous CO_2. The larger the relief diameter was, the longer the gas–liquid phase state lasted.

Keywords: Supercritical CO_2 release, pressure response, phase transition, small-scale pipeline

1 Introduction

One of the most difficult global environmental problems which human beings are now facing is the increasing atmospheric greenhouse gases and the resulting global warming [1]. CO_2 emitted from fossil fuel combustion is a major contributor to the greenhouse effect. This situation will not be changed in the coming decades due to the actual energy situation of the global energy structure [2]. Carbon capture and storage (CCS) technology intends to capture the released CO_2 at the emission sources, and transport the captured CO_2 to storage locations to mitigate the amount of CO_2 released into the atmosphere [3-5].

The scale and safety requirements of CCS application determine that pipeline transportation is the primary means of CO_2 transportation, due to its high efficiency and good economy [6, 7]. It is reported that a great deal of pipelines will need to be constructed in more densely populated areas, where multiple anthropogenic sources exist [8]. Pipelines usually suffer from failure risks, either puncture or full-bore rupture, caused by mechanical damage, corrosion, material defects, or operational error [9, 10]. After failure, CO_2 is released suddenly from the pipeline, causing property loss and casualties owing to asphyxia.

CO_2 released from pressurized pipelines is more complicated to deal with than other substances, because the CO_2 release process may include a combination of gaseous, liquid, and solid state CO_2 [11, 12]. During the CO_2 depressurization process after accidental release from an initially liquid or supercritical state to ambient conditions, the pressure and temperature drop

significantly owing to the expansion and subsequent high Joule–Thomson cooling effect, which causes the complex phase transition of CO_2 [13]. There have been several large research projects focusing on CO_2 release behaviour, including COOLTRANS [14], CO2PipeTrans [15], CO2PipeHaz [8], CO2QUEST [16], COSHER [17], and so on. This research is very helpful for understanding the safety issues related to CO_2 transportation.

Numerous publications have examined the release behaviour of CO_2 based on both experimental studies and numerical research. We have given a detailed introduction in our recently published works [18-22] and will therefore not repeat it in this article. Despite numerous studies nowadays, there is not yet a clear understanding of the pressure response and phase transition of the supercritical CO_2 depressurization process after accidental release from a pressurized pipeline. We performed an experimental study on the pressure response and phase transition of supercritical CO_2 during sudden release to improve the understanding of this process using a large-scale pipeline with a length of 258 m and an inner diameter of 233 mm from the CO2QUEST project, and found that the complex phenomena of pressure undershoot, rebound or slowdown occurred near the critical region [19, 20]. Moreover, we discussed the phase transitions of CO_2 in the pipeline at different diameters of relief orifices during the release process [21,22]. Medium-scale CO_2 release experiments were also performed to focus on the phases in the releases when supercritical and saturation CO_2 were released from a 5 m pipe connected to a 2 m^3 spherical vessel. Five stages with different depressurization rates and phase states were analyzed [23, 24]. However, these studies are far from sufficient.

With regard to the aforementioned problems, a study was proposed to focus on the pressure response and phase transition of supercritical CO_2 released from a small-scale

pressurized pipeline. High-frequency transducers were used to record the evolutions of fluid pressures during release. Thermocouples were placed to measure the temperatures of fluid.

2 Experiments

2.1 Experimental set-up

To investigate the pressure response and phase transition of supercritical CO_2 from a pipeline, a small-scale experimental facility was established [18]. The schematic diagram and photograph are shown in Figure 1. It consisted of a CO_2 insulated Dewar vessel, a 10 L buffer tank, a main pipe, a relief pipe, and a pneumatic valve driven by compressed air from a gas cylinder. CO_2 from the Dewar vessel was conditioned into the 10 L buffer tank, which was coated by a heat band which kept the CO_2 inside the buffer tank at the desired temperature, and glass wool insulation which kept the whole leakage process inside the buffer tank under a near-adiabatic condition.

A main pipe with an internal diameter of 25 mm and a length of 5 m was connected to the bottom of the buffer tank by an elbow. The other end of the main pipe was connected to a pneumatic valve. Several relief pipes with internal diameters of 25 mm and lengths of 1 m were machined before the experiments. These pipes were all closed at one end and each had a circular hole in the middle to simulate the leakage nozzle. When doing experiments, a selected relief pipe with the desired circular hole diameter was assembled to the pneumatic valve. Both the main pipe and relief pipe were coated by a heat band and glass wool insulation. The circular hole diameters in this study were 2 mm, 4 mm and 6 mm.

The pneumatic ball valve was DQ641Y type used in low temperature conditions. It could be used with the pressure less than 10 MPa and the temperature larger than -100 ℃. Its duration

time during value opening was about 0.1s~1s, depending on the actuating pressure.

Three pressure transducers labelled P_1, P_2, and P_3 and three armoured K-type thermocouples labelled T_1, T_2, T_3 were mounted at different locations along the main pipe to record the pressures and temperatures of CO_2 inside the main pipe, as shown in Figure 2. The accuracy and frequency of the pressure transducers were ±0.25% and 100 kHz. The response time and uncertainty of the thermocouples are 1 s and ± 1 °C. All sensors were calibrated before use. The data acquisition system was accomplished by the NI acquisition module and LabVIEW software [18-22].

2.2 Experiment procedure

The following steps are involved in each test: (1) Assembling the relief pipe with the desired hole diameter; (2) Examining the integrity of the whole pipeline set-up; (3) Debugging the testing instruments and data acquisition system; (4) Opening the atmospheric exhaust valve of the buffer tank, filling gas phase CO_2 from the Dewar vessel to the buffer tank for about 30 s, and then closing the exhaust valve and ending the filling process (keeping a pressure of 0.5 MPa in the buffer tank); (5) Filling liquid phase CO_2 from the Dewar vessel to the buffer tank. During this step, the evacuation of gas CO_2 in the buffer tank and the filling of liquid CO_2 to the buffer tank might be performed alternately. Experience was needed to judge the proper amount of CO_2 filled; (6) After the filling process, opening the heating system to make the pressure and temperature of CO_2 in the buffer tank meet the required experimental conditions. Evacuation might be needed in this step; (7) Opening the data acquisition system, setting up the image device; and activating the pneumatic valve; (8) Clearing up the experimental field.

Special attention was needed to safety issues during each step. Each test was repeated

several times (usually three) to ensure repeatable results within the permitted error range. All measurements were carried out under similar ambient temperature (about 15 °C) and humidity (about 60%). The initial pressure of 9 MPa and the initial temperature of 40 °C were selected in every experiment. Three relief diameters of the leakage nozzle were chosen: 2 mm, 4 mm, and 6 mm.

3 Results and discussions

3.1 Pressure and temperature evolutions in main pipe

Figure 3 shows the pressure evolutions at different locations inside the main pipe in the supercritical CO_2 release experiments with relief diameters of 2 mm (a), 4 mm (b), and 6 mm (c). In every subgraph, the release began at time t_1 when the pneumatic valve was activated. The pressures inside the main pipe underwent a sharp drop due to the expansion and release of supercritical CO_2 after the pneumatic valve was opened. The precipitous declines of pressure were slowed at time t_2. Apparently stable and gentle pressure drops appeared after t_2. After a period of time, the depressurization rate changes again at time t_3.

Based on the variation trend of the depressurization rate, three stages could be distinguished during every release process. The first stage was from time t_1 to time t_2. The durations were about 5.5717 s for 2 mm release diameter, 1.0365 s for 4 mm release diameter, and 0.752 s for 6 mm release diameter. The second stage was from time t_2 to time t_3. The durations were about 63.1628 s for 2 mm release diameter, 19.6248 s for 4 mm relief diameter, and 9.3560 s for 6 mm relief diameter. The third stage was from t_3 to the end time of the release. The different stages with various depressurization rates were attributed to the phase states of CO_2 inside the main pipe, which will be discussed in detail in the next section.

Moreover, the pressure curves were nearly synchronous at the testing locations P_1, P_2, and P_3 in each experiment. Though the pressure of P_3 was slightly greater than that of P_2, which was slightly greater than that of P_1, the pressure gradient from P_3 to P_1 was small. The synchronous changes of fluid pressures at different locations were similar to those tested in large-scale experimental pipelines with a length of 258 m and an inner diameter of 233 mm. However, no vapour bubbles and pressure rebound [19,20] were found in the small-scale experiments. Also, the propagation of decompression waves recorded in the large-scale experiments was harder to estimate in this study, probably because the experimental pipeline was too short.

Figure 4 shows the temperature evolutions at different locations inside the main pipe in the supercritical CO_2 release experiments with relief diameters of 2 mm (a), 4 mm (b), and 6 mm (c). Temperatures decreased just after the pneumatic valve was activated, due to the Joule–Thomson effect of the expansion process. Locations near the release orifice showed lower temperatures during the temperature decreasing process. But in these experiments, the temperature gradients were not very large. The largest temperature drops reached at location T_1 were about 38 °C for 2 mm relief diameter, 52 °C for 4 mm relief diameter, and 58 °C for 6 mm relief diameter. Larger relief diameters brought bigger temperature drops.

3.2 Phase transformation during release

Combining the tested pressure data with the temperature data at different times, we obtained the phase changes of CO_2 during the release process, as shown in Figure 5. After the pneumatic valve acted, the inventory properties inside the experimental main pipes (P_1, T_1; P_2, T_2; P_3, T_3) passed through the supercritical region and into the gaseous region of the phase diagram, due to the rapid pressure drop. Apparently, the supercritical state CO_2 was unlikely to change to

dense phase state because the pressure drop was more dominant than the temperature drop. Then the curves of all the measuring points tend to be close to the saturation line, which suggested that the unstable gaseous CO_2 quickly transformed into the gas–liquid phase. For a large part of the release, the measured pressures and temperatures of all locations followed approximately the saturation line. After a period of time along the saturation line, the pressure–temperature developments of all the testing points along the pipeline deviated from the saturation line, indicating that the gas–liquid phase CO_2 transformed into gaseous CO_2. The phase transition process was similar to those obtained in the large-scale experimental pipeline with a small release orifice [19] and medium-scale CO_2 releases with full bore rupture conditions [23].

The reason for the different depressurization rates in the different stages represented in Figure 3 can be explained as below. As shown in Figure 5, during the first stage from t_1 to t_2, the pressure drop was caused by the supercritical CO_2 release with a large depressurization rate. Then, during the second stage from t_2 to t_3, the supercritical CO_2 changed into gas–liquid phase CO_2, which slowed the depressurization rate of CO_2, due to the smaller density and larger compressibility of gas–liquid phase CO_2 than supercritical CO_2. Finally, during the third stage from t_3 to the release end, the pressure drop was attributed to the gas phase CO_2 release, during which the depressurization rate was different compared to the process of gas–liquid phase CO_2 release. In Figure 5, the valve acting time t_1, the first phase transformation time t_2, and the second phase transformation time t_3 were plotted. The corresponding pressures of t_1, t_2, and t_3 in Figure 5 were similar to those of t_1, t_2, and t_3 in Figure 3, demonstrating that the changes of the depressurization rate were related to the phase transformation.

3.3 Jet plume outside the relief orifice

High pressure CO_2 decompresses rapidly outside the leakage orifice, and experiences an expansion process, leading to a typical under-expanded plume in the dispersion process, which can be seen clearly as a white plume [25]. Figure 6 and Figure 7 show the appearance of jet dispersion at different times after release in the experiment with the relief diameters of 2 mm (Figure 7) and 4 mm (Figure 7). Due to the violent temperature drop caused by the J–T effect during the release process, the extremely low temperature (usually lower than -78 °C for supercritical CO_2 release) led to a phase change of CO_2 from other phase states to solid phase. As shown in Figure 6 and Figure 7, a compact core area inside the jet plume near the release orifice was formed, where a large fraction of solid CO_2 particles was generated. At 0 s after release (Figure 6a and Figure 7a), supercritical CO_2 in the pipe was released from the orifice. Then due to the transition from supercritical CO_2 to unstable gaseous CO_2 in the pipe, the dimensions of the jet plume decreased (Figure 6b, c, d and Figure 7b). Some time later, gaseous CO_2 in the pipe was transformed to gas–liquid phase, and the dimensions of the jet plume became larger and larger (Figure 6e, f and Figure 7c, d). After the gas–liquid phase CO_2 changed into gaseous CO_2 in the pipe, the dimensions of the jet plume gradually became smaller and invisible (Figure 6e, f and Figure 7 e).

3.4 Discussions

Recently we performed both larger-scale and small-scale supercritical CO_2 release experiments to study the pressure response and phase transition of CO_2 inside the experimental pipe [19-22]. Also, the results of medium-scale supercritical CO_2 release experiments can be found in the literature [23, 24]. There were both similarities and differences among the different scale release experiments.

First, the pressure responses during pipeline depressurization were different. The pressure undershoot, rebound or slowdown which occurred near the critical region in the large-scale experiments of supercritical CO_2 release [19,20] were not found in the medium-scale [23] and small-scale supercritical CO_2 release experiments. There may be a variety of possibilities for this difference, but the following two were the most likely reasons.

(1) In larger-scale CO_2 release experiments, the initiation of release was controlled by two blasting discs [19-22], which could be fully open in several millisecond. However, in small-scale CO_2 release experiments, the initiation of release was activated by a pneumatic ball valve, which had a much lower opening speed (nearly one second for fully opening). The faster the release orifice opened, the more severe the depressurization wave propagated and rebounded. Hence the pressure undershoot, rebound or slowdown would occur more easily in larger-scale experiments.

(2) In large-scale CO_2 release experiments, the pipe internal diameter of 243 mm was large enough that temperature gradient existed on the same cross section at the release onset [19-20]. However, in small-scale CO_2 release experiments, the internal diameter of the vent pipes was only 25 mm, and was too small to have temperature gradient on the same cross section. Hence the intense heat and mass transfers and the resulting pressure undershoot and rebound phenomenon occurred in the large-scale release experiments at the release onset were not seen in the small-scale experiments.

Second, the phase transitions of supercritical CO_2 during pipeline depressurization were similar [19, 23]. The initial supercritical CO_2 transformed into gaseous CO_2 (normally this stage was transient and unstable), followed immediately by the transformation of CO_2 into gas–liquid phase. After a period of time, the pressures and temperatures successively deviated from the saturation

line and the gas–liquid CO_2 transformed into gas phase.

4 Conclusions

This article has presented the results of a small-scale experimental investigation on the pressure response and phase transition of supercritical CO_2 release from a pressurized pipeline with a relief orifice. Some conclusions are demonstrated as follows:

(1) The pressure undershoot, rebound or slowdown which occurred near the critical region in the large-scale experiments of supercritical CO_2 release were not found in the small-scale supercritical CO_2 depressurization process.

(2) Locations near the release orifice reached lower temperatures during the temperature decreasing process. Larger relief diameters brought bigger temperature drops.

(3) Phase transitions occurred during the supercritical CO_2 release process. The supercritical CO_2 firstly turned into an unstable gas with a very great depressurization rate, then changed into the gas–liquid phase, and finally changed into gaseous CO_2.

(4) The larger the relief diameter was, the longer the gas–liquid phase lasted during the CO_2 release process.

(5) Both similarities and differences in the pressure responses and the phase transitions were found among the different scale release experiments.

Acknowledgement

The authors would like to acknowledge the funding received from the European Union Seventh Framework Programmes FP7- ENERGY-2009-1 under grant agreement number 241346 and FP7-ENERGY-2012-1STAGE under Grant agreement 309102.

References

[1] Putman WM, Ott L, Darmenov A, DaSilva A. A global perspective of atmospheric carbon dioxide concentrations. *Parallel Comput* 2016; 55:2–8.

[2] Myers SS, Wessells KR, Kloog I, Zanobetti A, Schwartz J. Effect of increased concentrations of atmospheric carbon dioxide on the global threat of zinc deficiency: a modelling study. *Lancet Glob Health* 2015; 3: 39-45

[3] Haszeldine RS. Carbon capture and storage: How green can black be?. *Science* 2009; 325: 1647–1652.

[4] Kanniche M, Gros-Bonnicard R, Jaud P, Valle-Marcos J, Amann J, Bouallou C. Pre-combustion, post combustion and oxy-combustion in thermal power plant for CO_2 capture. *Appl Therm Eng* 2010; 30: 53–62.

[5] Duan HB, Fan Y, Zhu L. What's the most cost-effective policy of CO2 targeted reduction: an application of aggregated economic technological model with CCS?. *Appl Energ* 2013; 112: 866–75.

[6] Munkejord ST, Hammer M, Løvseth SW. Intergovernmental panel on climate change, carbon capture & storage. *Appl Energ* 2016; 169: 499–523.

[7] Knoope MMJ, Ramirez A, Faaij APC. A state-of the-art review of techno-economic models predicting the costs of CO_2 pipeline transport. *Int J Greenh Gas Con* 2013; 16: 241–270

[8] Woolley RM, Fairweather M, Wareing CJ, Falle SAG, Mahgerefteh H, Martynov S, Brown S, Narasimhamurthy VD, Storvik IE, Saelen L, Skjold T, Economou IG, Tsangaris DM, Boulougouris GC, Diamantonis N, Custo L, Wardman M, Gant SE, Wilday J, Zhang YC, Chen SY, Proust C, Hebrard J, Jamois D. CO_2PipeHaz: Quantitative hazard assessment for next generation CO_2 pipelines. *Energy Procedia* 2014; 63: 2510–2529.

[9] Koornneef J, Spruijt M, Molag M, Ramirez A, Turkenburg W, Faaij A. Quantitative risk assessment of CO_2 transport by pipelines – A review of uncertainties and their impacts. *J Hazard Mater* 2010; 177: 12–27.

[10] Duncan IJ, Wang H. Estimating the likelihood of pipeline failure in CO_2 transmission pipelines: New insights on risks of carbon capture and storage. *Int J Greenh Gas Con* 2014; 21: 49–60

[11] Elshahomi A, Lu C, Michal G, Liu X, Godbole A, Venton P. Decompression wave speed in CO2 mixtures: CFD modelling with the GERG-2008 equation of state. *Appl Energ* 2015; 140: 20–32.

[12] Hill TA, Fackrell JE, Dubal MR, Stiff SM. Understanding the consequences of CO_2 leakage downstream of the capture plant. *Energy Procedia* 2011; 4: 2230–2237.

[13] Mazzoldi A, Hill T, Colls JJ, Assessing the risk for CO_2 transportation within CCS projects, CFD modelling. *Int J Greenh Gas Con* 2011; 5: 816–825.

[14] Copper R. National grid's COOLTRANS research programme. *J Pipel Eng* 2012; 11: 155–172.

[15] Brown J, Holt H, Helle K. Large scale CO_2 releases for dispersion model and safety study validation. *Energy Procedia* 2014; 63: 2542–2546.

[16] Brown S, Martynov S, Mahgerefteh H, Fairweather M, Woolley RM, Wareing CJ, Falle SAG, Rutters H, Niemi A, Zhang YC, Chen SY, Besnebat J, Shah N, Dowell NM, Proust C, Farret R, Economou IG, Tsangaris DM, Boulougouris GC, Wittenberghe JV. CO_2QUEST: Techno-economic assessment of CO_2 quality effects on its storage and transport. *Energy Procedia* 2014; 63: 2622–2629.

[17] Ahmad M, Lowesmith B, Koeijer GD, Nilsen S, Tonda H, Sponelli C, Cooper R, Clausen S, Mendes R, Florisson O. COSHER joint industry project: Large scale pipeline rupture tests to

study CO_2 release and dispersion. *Int J Greenh Gas Con* 2015; 37: 340–353.

[18] Yan X, Guo X, Liu Z, Yu J. Release and dispersion behavior of carbon dioxide released from a small-scale underground pipeline, *J Loss Prevent Proc* 2016; 43: 165-173

[19] Guo X, Yan X, Yu J, Zhang Y, Chen S, Mahgerefteh H, Martynov S, Collard A, Proust C. Pressure responses and phase transitions during the release of high pressure CO2 from a large-scale pipeline. *Energy* 2017; 118: 1066-1078.

[20] Guo X, Yan X, Yu J, Zhang Y, Chen S, Mahgerefteh H, Martynov S, Collard A, Proust C. Pressure response and phase transition in supercritical CO2 releases from a large-scale pipeline. *Appl Energ* 2016; 178: 189-197.

[21] Guo X, Yan X, Yu J, Zhang Y, Chen S, Mahgerefteh H, Martynov S, Collard A, Proust C. Under-expanded jets and dispersion in high pressure CO2 releases from an industrial scale pipeline. *Energy* 2017; 119: 53-66.

[22] Guo X, Yan X, Yu J, Zhang Y, Chen S, Mahgerefteh H, Martynov S, Collard A, Proust C. Under-expanded jets and dispersion in supercritical CO2 releases from a large-scale pipeline, *Appl Energ* 2016; 183: 1279-1291.

[23] Hebrard J, Jamois D, Proust C, Spruijt M, Hulsbosch-Dam CEC, Molag M, Messina E. Medium scale CO2 releases. *Energy Procedia* 2016; 86: 479-488

[24] Jamois D, Proust C, Hebrard J. Hardware and instrumentation to investigate massive releases of dense phase CO2. *Can J Chem Eng* 2015; 93: 234-240.

[25] Li K, Zhou X, Tu R, Xie Q, Yi J, Jiang X. An experimental investigation of supercritical CO2 accidental release from a pressurized pipeline. *J Supercrit Fluid* 2016; 107: 298-306

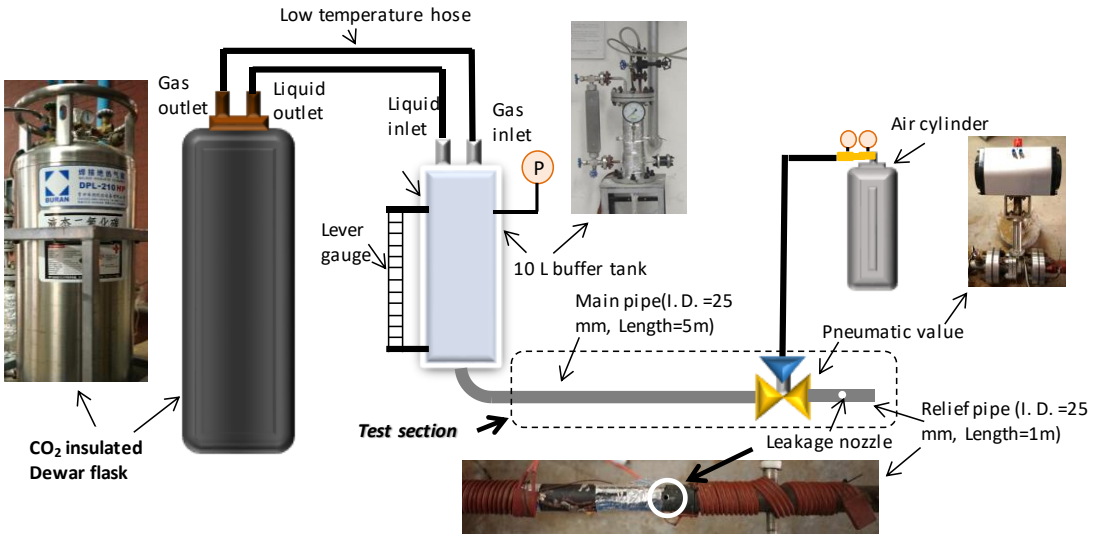

Figure 1 Schematic diagram of the supercritical phase CO_2 release experimental set-up

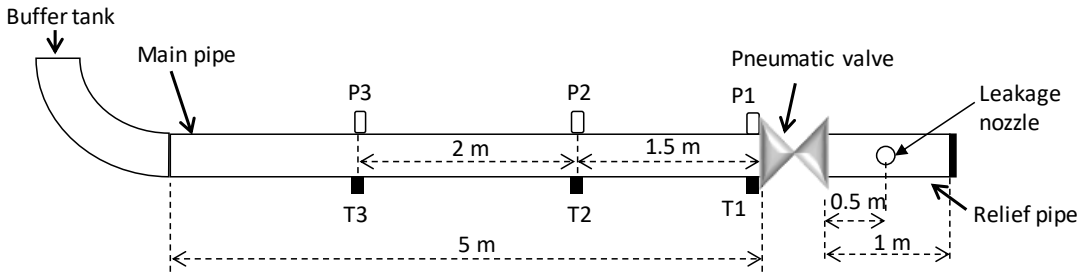

Figure 2 Schematic diagram of the leakage nozzle and testing locations on relief pipe and main pipe

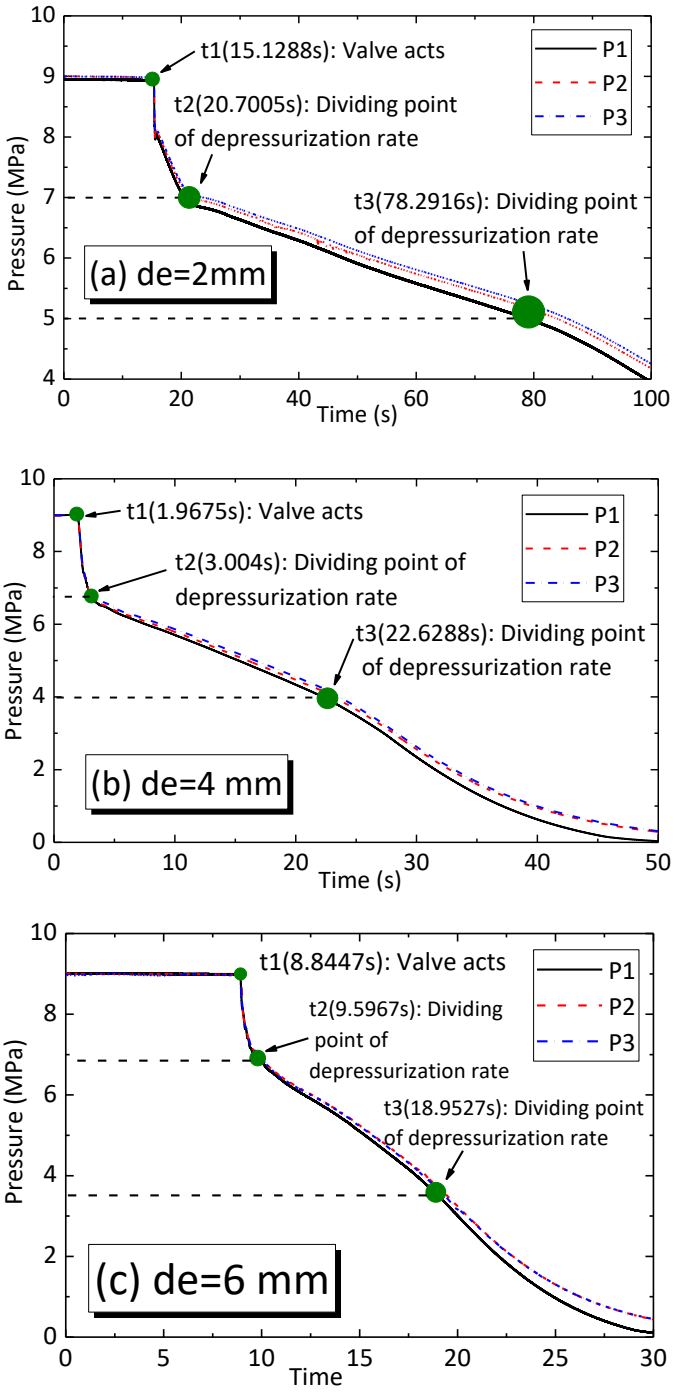

Figure 3 Pressure evolutions of the supercritical CO_2 release experiments with different relief diameters (initial pressure of 9 MPa, initial temperature of 40 °C).

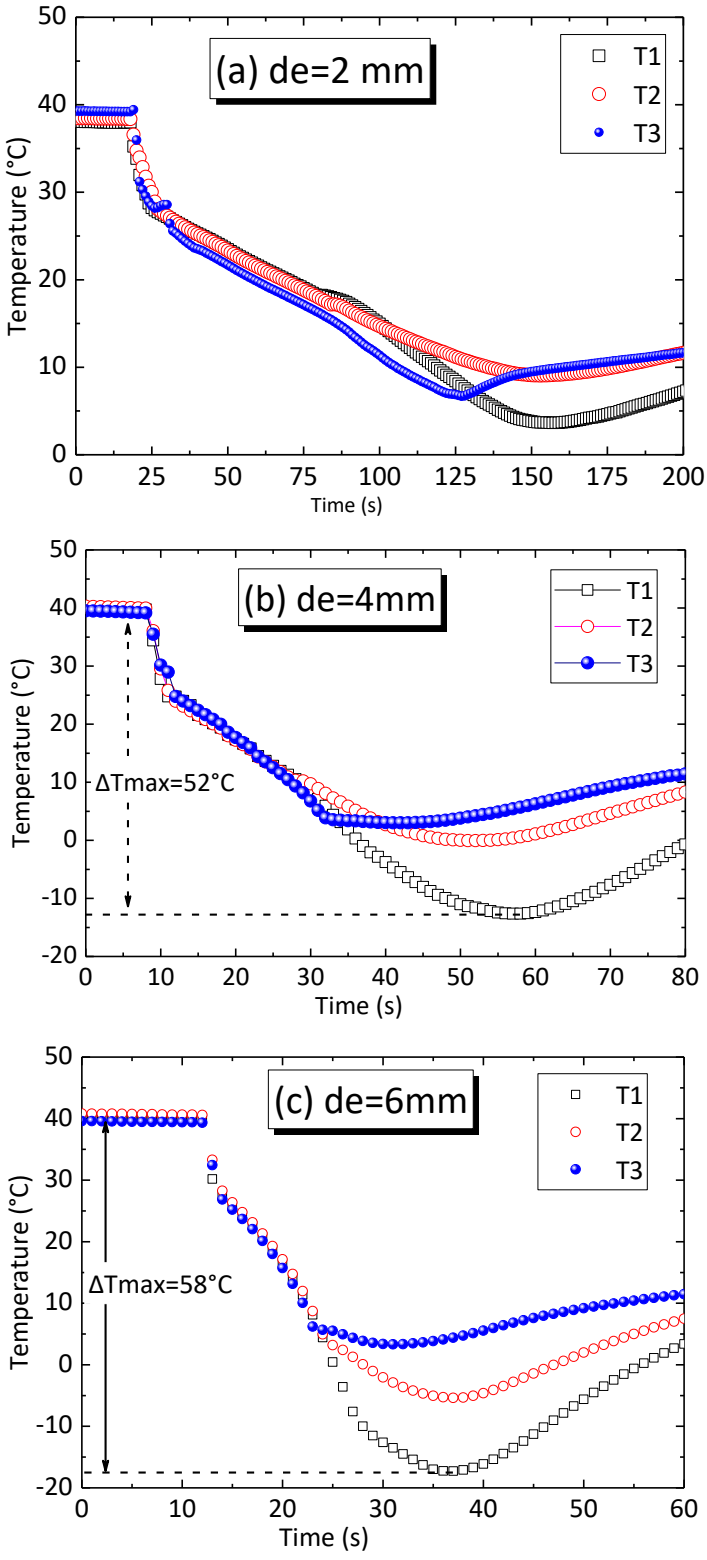

Figure 4 Pressure and temperature evolutions of the supercritical CO_2 release experiments with different relief diameters (initial pressure of 9 MPa, initial temperature of 40 °C).

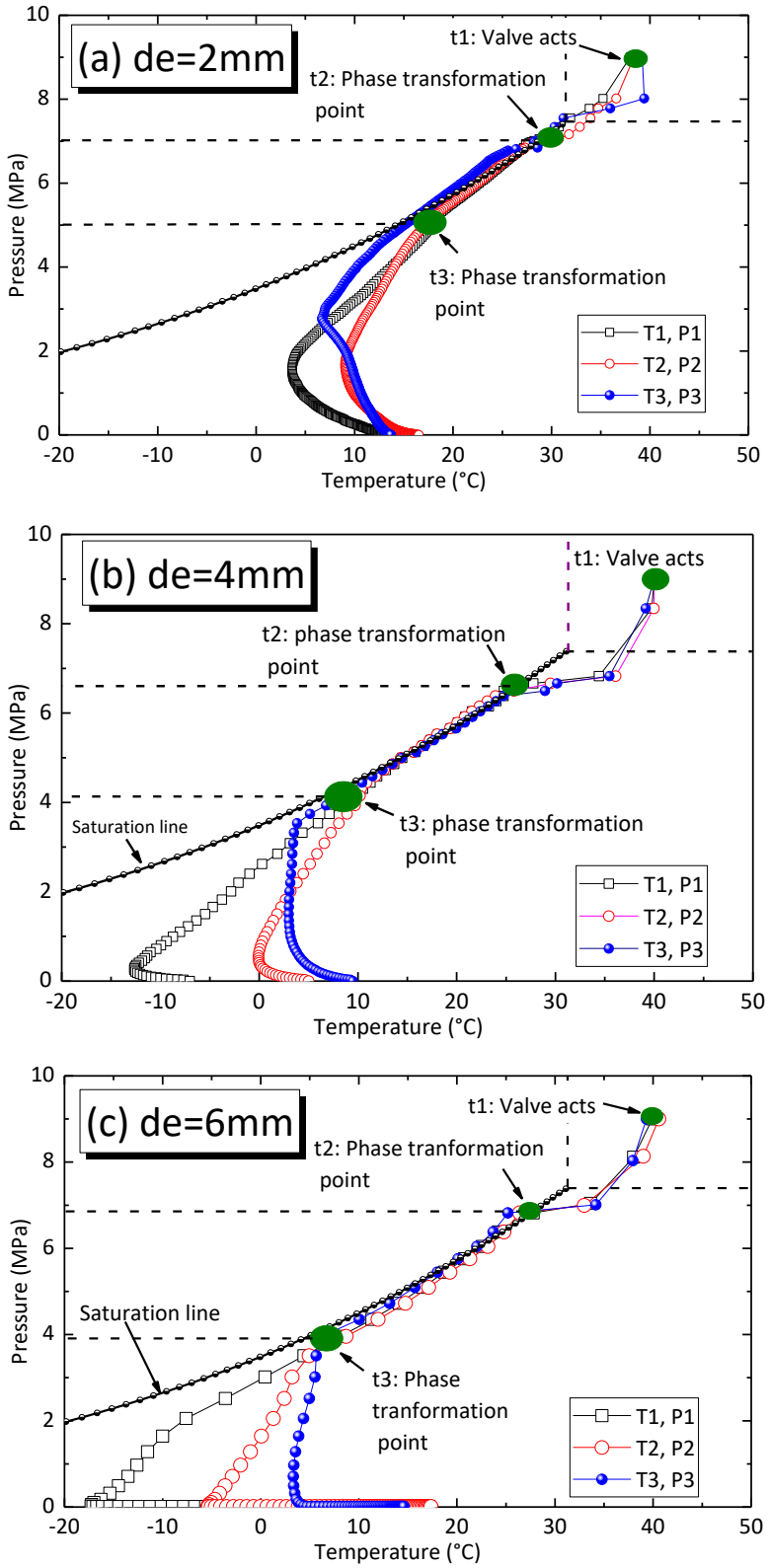

Figure 5 Pressures-temperature development of the supercritical CO_2 release experiments (initial pressure of 9 MPa, initial temperature of 40 °C).

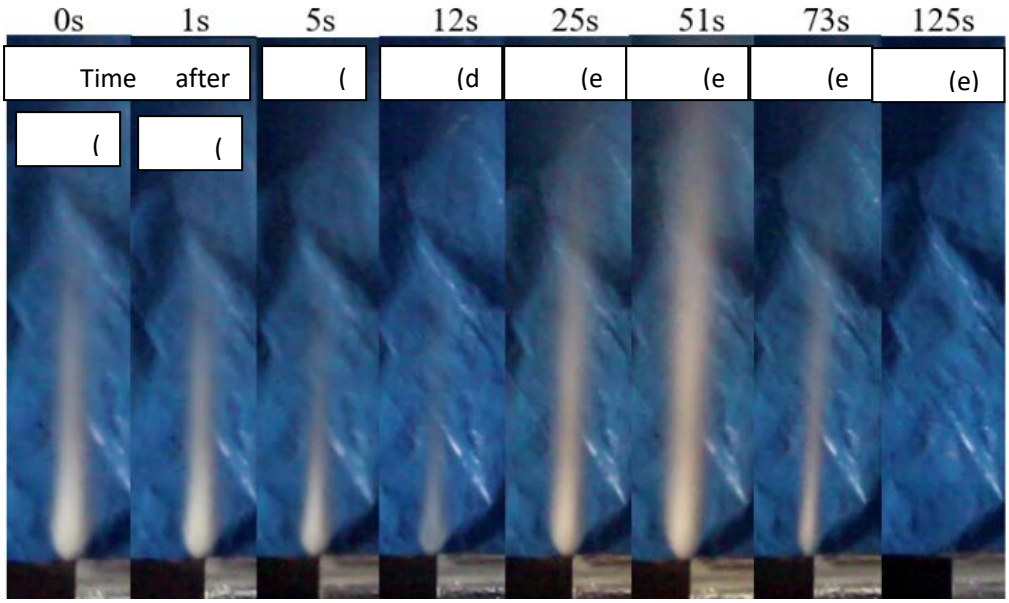

Figure 6 Jet flow phenomena (initial pressure of 9 MPa, initial temperature of 40 °C, and leakage hole diameter of 2 mm)

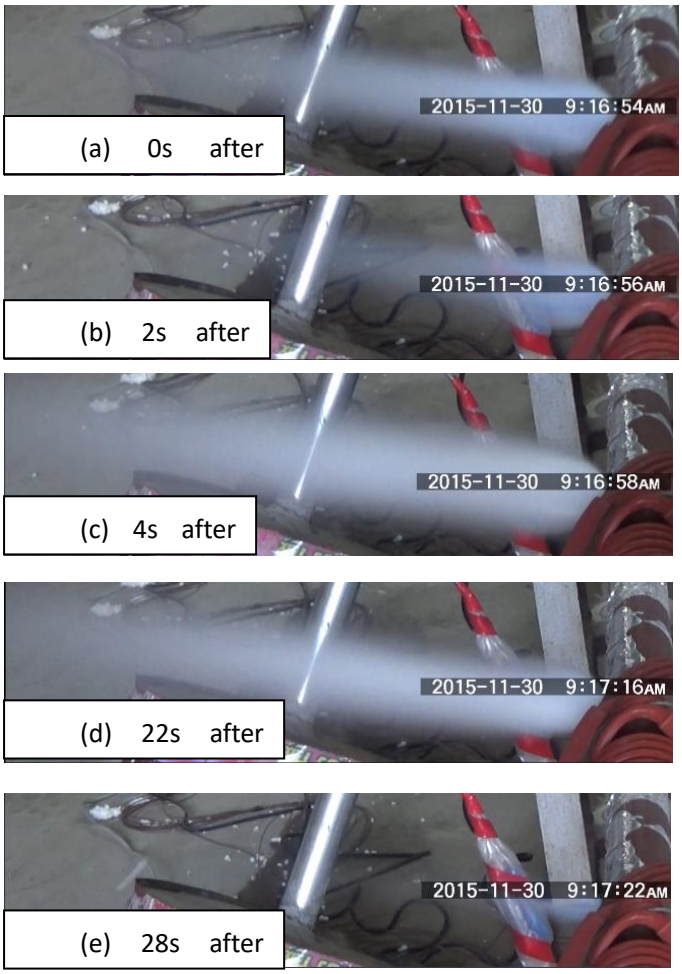

Figure 7 Jet flow phenomena (initial pressure of 9 MPa, initial temperature of 40 °C, and leakage hole diameter of 4 mm).